



Multiobjective Optimization of Beam Structure for Bogie Frame Considering Fatigue-Life Extension

Seokheum Baek¹ · Xueguan Song² · Myungil Kim³ · Jaesung Kim⁴

Received: 19 October 2020 / Revised: 4 January 2021 / Accepted: 11 January 2021 / Published online: 18 February 2021
© The Korean Institute of Electrical Engineers 2021

Abstract

This paper addresses the multiobjective optimization of a brake end beam of a bogie frame with consideration of three elements: the stress, fatigue, and weight. A finite-element analysis (FEA) is performed to obtain the stress distribution of the component, and the stress-life method and fatigue notch factor are used for fatigue-life assessment based on the FEA results. Subsequently, the multiobjective optimization problem in the form of mathematical functions, which considers three objectives, is handled using the design of experiments, approximation technique, analysis of variance, multiobjective algorithm, and Pareto-optimal solution. Finally, the FEA is validated according to the optimal result to verify the accuracy of the optimization. The results of this study indicate that the proposed approach is very available and has potential for the optimal design of the components of the bogie frame and/or the bogie itself.

Keywords Fatigue optimization · Bogie frame · Notch effect · Chebyshev polynomial model · Goal programming

1 Introduction

A bogie is a basic assembly that is needed for railway carriages/cars and locomotives. It serves many purposes, e.g., providing support of the rail vehicle body, providing stability on both straight and curved tracks, and ensuring ride comfort by absorbing vibration [1]. As shown in Fig. 1, a typical bogie includes several key components: the bogie frame, the suspension system to absorb shocks between the bogie frame and the rail vehicle body, two wheelsets composed of two axles with bearings and a wheel at each end, an axle box suspension to absorb shocks between the axle bearings and the bogie frame, brake equipment, and traction motors.

As the framework, the bogie frame significantly affects the vehicle safety, running performance, and ride quality.

It is usually designed and manufactured to serve for a long time; thus, sufficient static strength and fatigue life must be ensured, as well as sufficient static strength under static and dynamic loading conditions. In traditional design, they can only be tested after the bogie frame is built as a real physical hardware; the design and test will not stop until the bogie frame satisfies all the engineering requirements. Currently, with the demand for shorter product cycles and the development of numerical methods and computer technology, the finite-element method (FEM) has been widely used in the design of bogie frames, particularly the estimation of the stress and fatigue life.

2 Related Works

Over the past decades, many studies have been performed on the stress and fatigue analysis in the design of bogies and relative welded products. In 1998, Dietz et al. [2] presented a new approach for predicting the fatigue lifetime of the bogie of a freight locomotive. It is based on the combination of frequency- and time-domain calculations and is implemented together with a computer-aided design, an FEM, and a multi-body system program. Oyan [3] conducted a finite-element analysis (FEA) of the bogie frame in Taipei rapid transit systems to confirm the technical strength requirements for

✉ Jaesung Kim
jaesungkim@hanbat.ac.kr

¹ CAE Team, DNDE Inc., Busan, South Korea

² School of Mechanical Engineering, Dalian University of Technology, Dalian, China

³ Supercomputing Modeling and Simulation Center, Korea Institute of Science and Technology Information, Daejeon, South Korea

⁴ Department of Industry-Academic Convergence, Hanbat National University, Daejeon, South Korea

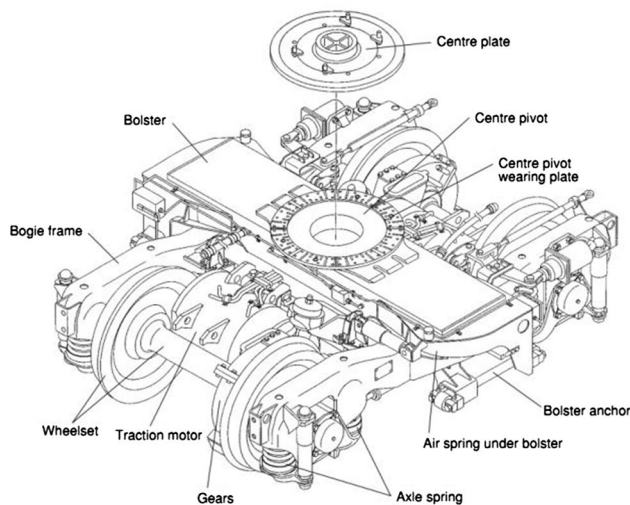


Fig. 1 Structure of a typical bogie

static and dynamic loadings. The von Mises stresses were adopted as equivalent stresses in the static strength calculation, and the principal stresses were adopted in the fatigue-strength evaluation. In 2000, Ferguson [4] analyzed the bogie using FEMs to cover the lower-frequency range. The wagon has been analyzed using a statistical energy analysis approach. In 2007, the structural safety of a tilting bolster was investigated via experiments and FEAs by Kim et al. [5]. The structural safety of the bolster frame was evaluated via a static test under static loads, and the fatigue strength was assessed using a Goodman diagram. Baek et al. [6] predicted the fatigue life of an end beam in a freight car bogie by using the rainflow cycle counting method. The fatigue life calculated via the rainflow cycle counting method, the P–S–N curve, and the modified Miner’s rule agreed well with the actual fatigue life. Two- and three-dimensional finite-element simulations of the T-type fillet weld frequently used in the heavy vehicle machine industry were performed by Barsoum and Lundback [7]. The residual stress predicted via FEA agrees well with measurements and hence is suitable for residual stress predictions and for incorporation in further fatigue crack growth analysis. Kim and Yoon [8, 9] investigated the static behaviors and fatigue strength of a glass fiber-reinforced plastic (GFRP) composite bogie frame for urban subway trains under critical load conditions. The stress and strain distribution for the whole bogie frame was evaluated through FEA and compared with the experimental results. The fatigue strength of the bogie frame was evaluated using a Goodman diagram according to JIS E4207. Various fatigue assessment methods were applied to the vertical main loading of a bogie frame for a light rail vehicle by Kassner [10]. Comparative stress analyses for selected stress points indicated the potential and advantages of fatigue assessment with the real loading assumptions and

with different evaluation methods. A fatigue-strength analysis of welded joints in closed steel sections in rail vehicles was performed by Esdert et al. [11]. The applicability of the notch stress concept to the fatigue design of typical, line welded, closed section steel parts (which are used in railway vehicle construction) was analyzed and improved.

Fatigue optimization began in the early 1970s [12] and was extensively applied to railway structures. Park [13] presented a paper addressing the optimum design of the tilting bogie frame with consideration of the fatigue strength and weight. An FEA was performed to calculate the stress distribution and fatigue strength of the bogie frame. An artificial neural network was used to approximate the function, and a genetic algorithm (GA) was used for optimization. Wang et al. [14] used the stochastic response surface method to predict the relationship between the fatigue life and the load capacity coefficient in the standard Gaussian space. Mrzygłob and Zielinski [15, 16] conducted research on parametric structural optimization with respect to the multiaxial high-cycle fatigue criterion. The work focused on three principle areas: the fatigue of the material, parametric optimization of the structures, and application of the FEM. In the computational examples, the proposed optimization methodology allowed the mass of the studied structure to be significantly reduced while its durability was maintained at an established level. Similarly, Song et al. [17] optimized a control arm in an automotive suspension with consideration of the static strength and fatigue life by using the metamodel method. Two metamodels were used for the approximation of the objective functions. Bosnjak et al. [18] performed failure analysis and redesign of the bucket wheel excavator two-wheel bogie. The cause of the failure was first discussed, and then the two-wheel bogie was redesigned to satisfy the strength criterion.

Despite the foregoing significant research, the bogie frame design remains a complex and multidisciplinary task (particularly with the high demand for lightweight structures for saving energy) where the structural factors, fatigue, weight, and many other aspects must be taken into account simultaneously, leading to a very challenging problem for designers. For instance, numerous different calculations are necessary for the strength assessment, which are computationally expensive. The loading condition on the bogie frame is random and complex to derive; although there are international standards, many assumptions must be made. The stress, fatigue, weight, and other factors cannot be expressed as an analytical function in terms of the design variables, making the optimization impracticable. Additionally, designers cannot identify a single solution that simultaneously optimizes two or more conflicting objectives, such as maximizing the fatigue life and minimizing the weight of the bogie frame.

To resolve all the difficulties, the FEA and multiobjective optimization technique, including the Chebyshev orthogonal polynomial model and the multiobjective optimization algorithm, should be utilized for the optimal design of the bogie frame satisfying many imposed requirements. In this study, multiobjective optimization considering the static strength, fatigue strength, and weight reduction for the brake end beam in the bogie frame design is examined. FEAs of the end beam and bogie frame are performed to derive the static strength and distribution, and the notch stress is used for fatigue assessment. The optimization problem has three objectives: maximizing the fatigue life and minimizing the maximum stress and weight of an end beam in the bogie frame. Specially, the Chebyshev orthogonal polynomial model is used to construct response surface approximations for the stress, fatigue life, and weight of the bogie frames with complex geometries and/or loading conditions. Compromise decision support problem formulation is utilized for the multiobjective optimization. After the optimization, a stress and fatigue analysis is performed to verify the optimal design.

3 Method of Fatigue Analysis

3.1 Material Properties

The bogie frame comprises several parts, such as end beams, side beams, and cross beams, which are made of two types of materials. The brake end beams considered in this study are made of SS400, and the other parts (including the cross beams and side beams) are made of SM490A, which have a higher strength than SS400. For the fatigue data, extensive testing of 10-mm-thick flat specimens of SS400 was conducted under alternating bending stresses ($R = 1$) in a previous study [6], and the results were used in the present study even though the geometry of the brake end beam was significantly different from that of the specimens. Figure 2 plots the fatigue-life curves of SS400 with 5%, 50%, and 95% probability of failure. To account for uncertainties, the average fatigue-life curve, i.e., that with 50% probability of failure, was used; thus, the fatigue life N_f can be modeled as a function of the stress level:

$$\log N_f = 6.728 - 0.094S_f/2 \pm 0.405 \tag{1}$$

where S_f represents the failure stress, and the mean of the fatigue limit obtained via the JSME statistical S–N testing method is 52.8 MPa.

3.2 Fatigue-Life Calculation

Many methods have been used to assess the fatigue lives of structures over the years. However, most of the fatigue calculations in engineering are based on the three-core method, i.e., the stress-life, strain-life, and crack-propagation methods.

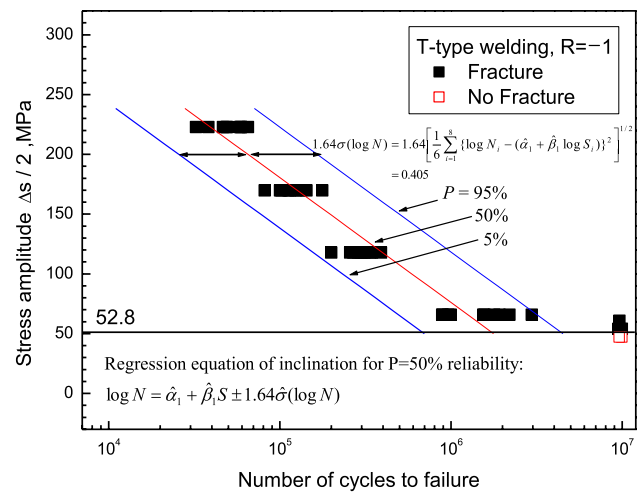


Fig. 2 P–S–N curve for SS400 alloys

The first two methods do not model the crack growth process, and the third one deals with crack propagation and relies on the initial crack. In this study, the first method, i.e., the stress-life method, is used, because the stress at any location within a model can be determined easily via FEA. Furthermore, because the virtual bogie frame contains notches in one form or another, the treatment of the fatigue notch must be taken into account for estimating the effect of the weld geometry.

Almost all machine components and structures contain stress concentrators, which can cause cracks to form. The theoretical stress concentration depends on the geometry and the mode of loading (axial, in-plane bending, etc.) and relates through a stress concentration factor defined in Eq. (2).

$$K_t = \frac{S_{\max}}{S} \tag{2}$$

Here, S_{\max} represents the local maximum stress, and S represents the nominal or average stress. This is a useful way to describe the stress concentration. However, when a notch exists, the stress field becomes a singularity, and the stress concentration factor, K_t , is no longer an effective way of describing the feature. Instead, the fatigue notch factor (also called the fatigue stress concentration factor) K_f is introduced to describe the intensity of the stress field around the singularity.

$$K_f = q(K_t - 1) + 1 \tag{3}$$

Here, q is the notch sensitivity factor containing the material parameter with a unit of length C and notch root radius r .

$$q = \frac{1}{1 + C/r} \tag{4}$$

The value of q varies from 0 (corresponding to no influence of K_t) to 1 (corresponding to a full contribution). For

ferrous-based wrought metals, the constant C is given as follows:

$$C \approx \left(\frac{300}{S_u(\text{ksi})} \right)^{1.8} \text{ inch} \approx \left(\frac{300}{0.5BHN} \right)^{1.8} \text{ inch}, \quad (5)$$

where S_u represents the tensile yield stress in units of ksi, and BHN represents the Brinell hardness number of the material. Hence, the real stress value, S_f , including the notch influence can be corrected as follows:

$$S_f = S'_f \times K_f, \quad (6)$$

where S'_f represents the stress values measured in experiments or obtained from the FEA.

3.3 FEA

Figure 3 shows the real bogie frame, including the end beam and the failure location of the end beam. The welded bogie frame of the freight locomotive is approximately 3.5 m long and 2.4 m wide, and its mass is approximately 2200 kg. The fatigue fractures of the end beam occur at the end of the welding zone between the beam with a C-shaped end and the gusset plate.

As mentioned previously, the objective of this study was to develop a multiobjective optimization method considering the stress, fatigue, and weight for the brake end beam in the bogie frame. To obtain high-fidelity results, half of the entire bogie frame including the brake end beam and other main parts were modeled for the FEA, as shown in Fig. 4. The model was first constructed in CATIA and then imported into ANSYS for the generation of the finite-element model and the next simulation. The model was freely meshed with 10-node tetrahedral elements (SOLID88, which is generally regarded as a good element type for generating high-quality meshes for complex structures). The mesh sizes were compared to avoid mesh sensitivity and determine the appropriate element size with appropriate accuracy. Because the braking system was ignored in the model, 2-node beam elements (BEAM4) and coupling elements were used to model the load applied to the bracket hinge of the end beam, which was simpler and faster than the nonlinear contact analysis between two bodies. The corresponding finite-element model (ANSYS) consists of 275,027 finite elements and 529,136 nodes.

As shown in Fig. 4, the gravitational acceleration was considered, and the load condition was in accordance with JIS E4207 (1984) [19]. The main loads acting on the bogie frame, i.e., the vertical load of 17,000 kg (Force9) and braking load of 2875 kg (Force10), were applied to center pivot and end beam, respectively. Additionally, special boundary conditions were considered, as follows:



Fig. 3 Bogie frame of the freight train and its fracture at the end beam

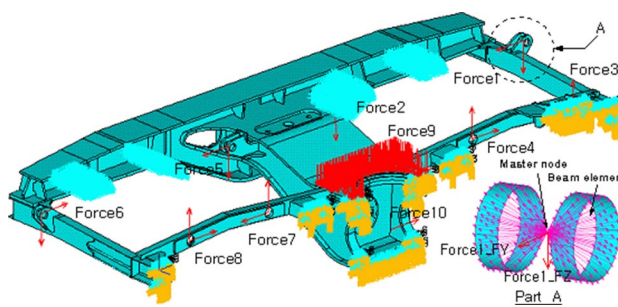


Fig. 4 Bogie frame model with coupled effects of the load and boundary conditions

- The side frame suspension displacements were fixed in the three axial directions.
- The braking load arose from the friction between the wheel tread and the brake pad.
- The longitudinal load was 30% of the static vertical load.
- The transverse load was 40% of the static vertical load.

Figure 5 illustrates the von-Mises stress distribution on the bogie frame under the typical braking load condition, the

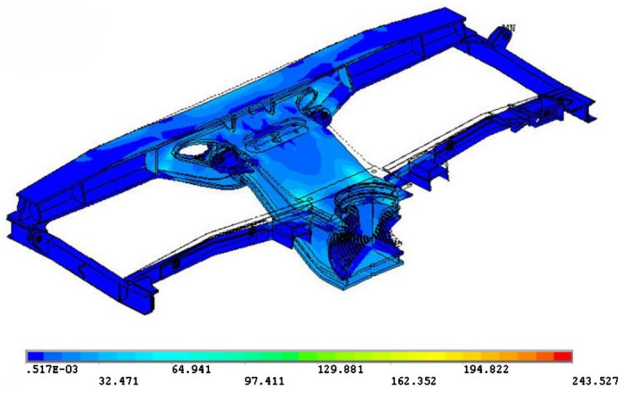


Fig. 5 Stress distribution of the bogie frame

center pivot experienced the highest stress (approximately 243.5 MPa), and there was no stress concentration in the connection of the bogie frame with end beam. As shown in Fig. 6, the maximum von-Mises stress for the end beam (75.4 MPa) occurred at the corner of the welded gusset plate, where accidents due to fatigue failure occurred. A fatigue crack was initiated again in this region after the reinforced end beam was installed at the bogie frame.

The high level of stress in the end beam area was the main reason for crack initiation. The fatigue loads (combination of the self-weight and braking load) caused the successive propagation of the crack to the critical size, leading to rupture in the welded gusset plate. A significantly lower value of stress in the region of the side frame is observed in Fig. 5. Except for the center pivot, the center frame was not as highly loaded as the end beam. The maximum von-Mises stress in the region of the center frame was only 243.5 MPa, whereas in the side frame, the stresses were in the range of 112.2 MPa.

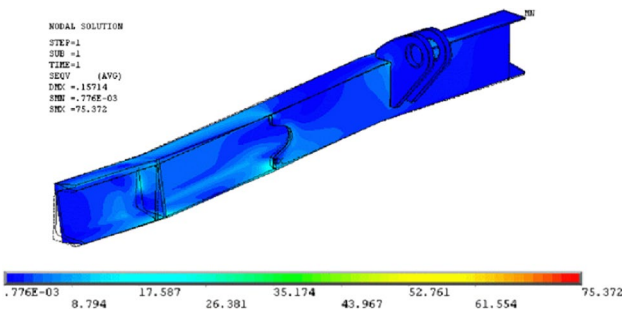


Fig. 6 Stress distribution of the end beam with a braking load

4 Fatigue Optimization Method

4.1 Chebyshev Polynomials Approximation Model

Clearly, the stress and fatigue, as well as the weight of the brake end beam, are nonlinear and cannot be formulated analytically, owing to the complexity of the structures. This is the main challenge for the subsequent optimization. The Chebyshev polynomial response model is effective for formulating the relationship between the aforementioned properties and the design variables.

The Chebyshev polynomial response model, which is named after Pafnuty Chebyshev, features a sequence of orthogonal polynomials that are related to de Moivre’s formula and can be defined recursively. Mathematically, the exact functional relationship can be approximated as follows:

$$y = b_0 + b_1(x - \bar{x}) + b_2 \left[(x - \bar{x})^2 - \frac{a^2 - 1}{12} h \right] + b_3 \left[(x - \bar{x})^3 - \frac{3a^2 - 7}{20} (x - \bar{x}) h^2 \right] + b_n p_n(x), \tag{7}$$

where $p_n(x)$ represents the basis functions that are dependent on the design variables (x).

$$p_0(x) = 1, \quad n = 0$$

$$p_1(x) = x - \bar{x}, \quad n = 1$$

$$p_2(x) = (x - \bar{x})^2 - \frac{(a^2 - 1)}{12} h^2, \quad n = 2$$

$$p_n(x) = p_{n-1}(x)p_1(x) - \left[\frac{(n-1)^2 \{a^2 - (n-1)^2\}}{4\{4(n-1)^2 - 1\}} \right] h^2 p_{n-2}(x), \quad n = 3, 4, 5, \dots$$

Here, \bar{x} represents the average value of the design variable, a represents the level number, and h is the coefficient of the level interval. The order should be less than the level number, and the maximum order of the design variable is $a - 1$. The coefficients of regression b_0 and b_i are expressed by Eqs. (8) and (9), respectively.

$$b_0 = T/lm = \bar{y} \tag{8}$$

$$b_i = \frac{\sum_{k=1}^a p_i(x_k) y_k / \sum_{k=1}^a p_i^2(x_k)}, \quad k = 1, 2, \dots, a \tag{9}$$

where x_k in $p_i(x_k)$ represents the level number for each x , and y_k represents the analysis average of each level. The advantage of the orthogonal polynomial is that it allows the analysis of variance (ANOVA). The use of the ANOVA with the orthogonal polynomial allows the total variance of the response to be divided into the 1st-, 2nd-, and n -1th-order components. Thus, it is possible to judge the appropriate maximum order by estimating the co-relationship and sensitivity.

4.2 Design of Experiments (DOE)

For formulating the objective functions, sample points are needed to explore the design space. A typical method for generating sample points is DOE. Among the many different DOEs, D-optimal design is considered to be effective for addressing the limitations of traditional designs, as it is expensive or infeasible to measure the combinations of factor levels for nonlinear models [20–22]. D-optimal designs do not require orthogonal design matrices. They are generated by an iterative search algorithm and seek to minimize the covariance of the parameter estimates for a specified model. This is equivalent to maximizing the determinant $D=|X^T X|$, where X represents the design matrix of model terms (the columns) evaluated at specific treatments in the design space (the rows).

4.3 ANOVA

After the approximate models are obtained, it is essential to examine the fitted or approximate model if the model provides an adequate approximation of the true response surface. In this case, a classical ANOVA of the regression is used to examine the accuracy of the fitted models. Table 1 presents detailed information such as the sum of squares of the model, DOF, mean square, and statistical hypothesis (F-statistics) [23].

SSR, SSE, SST, and R^2 are defined as follows:

$$SSR = \sum_{i=1}^N (\hat{Y}_i - \bar{Y}_i)^2 \tag{10}$$

$$SSE = \sum_{i=1}^N (\hat{Y}_i - Y_i)^2 \tag{11}$$

$$SST = \sum_{i=1}^N (Y_i - \bar{Y}_i)^2 \tag{12}$$

$$R^2 = \frac{SSR}{SST} = \frac{\sum_{i=1}^N (\hat{Y}_i - \bar{Y}_i)^2}{\sum_{i=1}^N (Y_i - \bar{Y}_i)^2}, \tag{13}$$

where Y are the mean of, respectively.

4.4 Optimization Algorithm

The objective of this study was to optimize the end beam structure for improving its safety and weight in terms of different criteria simultaneously. Numerous multiobjective optimization methods and algorithms have been proposed. Among them, typical ones include multiobjective GAs, the weighted-sum method, the weighted min–max method, the lexicographic method, the bounded objective function method, and the goal programming (GP) method [24]. Each of these multiobjective optimization methods has advantages and disadvantages. For example, multiobjective GAs explore all the objectives independently and simultaneously to search for the so-called Pareto-optimal set, but these algorithms are expensive and take too much computation time. The weighted-sum method formulates different objective functions into a single objective function with alterable weight coefficients, and then a standard single-objective optimization routine is used to solve the consequent formulation. This method is simple, but its limitation is apparent. It is impossible to know the correct weights needed to generate points evenly spread on the Pareto curve without knowing the shape of the Pareto curve [25]. Hence, deciding which one is most appropriate or most effective can be difficult and/or unpractical. It depends on the nature of the user’s preferences and what type of solution might be acceptable [26]. In this study, the GP method was adopted for multiobjective optimization.

GP [27, 28] is a branch of multiobjective optimization, which in turn is a branch of multi-criteria decision analysis (also known as multiple-criteria decision making). GP allows several objectives to be considered simultaneously in a problem for choosing the most satisfactory solution within a set of feasible solutions. More precisely, the GP finds a solution that minimizes the deviations between the

Table 1 ANOVA results

Source of variation	Sum of squares (SS)	DOF	Mean square (MS)	F-ratio (F)
Due to regression	SSR	$p - 1$	$SSR/(p - 1)$	$SSR (p - 1)/SSE(N-p)$
Residual	SSE	$N - p$	$SSE/(N - p)$	
Total	SST	$N - 1$		

achievement level of the objectives and the goals set for them in the order arranged according to the function’s importance. With GP, goals (f_j^*) are specified for each objective function $f_j(\mathbf{X})$. Then, the total deviation $\sum_{j=1}^k |d_j|$ from the goals is minimized, where d_j represents the deviation from the goal b_j defined by the decision maker. d_j is split into positive and negative parts such that $d_j = d_j^+ - d_j^-$ with $d_j^+ \geq 0$, $d_j^- \geq 0$, and $d_j^+ d_j^- = 0$. Consequently, $|d_j| = d_j^+ d_j^-$, where d_j^+ and d_j^- represent underachievement and overachievement, respectively, and are defined as follows:

$$\begin{aligned} d_j^+ &= \max \left[0, f_j(\mathbf{X}) - f_j^* \right] & d_j^+ &= \frac{1}{2} \left[|f_j^* - f_j(\mathbf{X})| + f_j(\mathbf{X}) - f_j^* \right] \\ d_j^- &= \max \left[0, f_j^* - f_j(\mathbf{X}) \right] & d_j^- &= \frac{1}{2} \left[|f_j^* - f_j(\mathbf{X})| + f_j^* - f_j(\mathbf{X}) \right] \end{aligned} \tag{14}$$

Therefore, the optimization problem is modified as follows:

$$\begin{aligned} \text{Min} : & \sum_{j=1}^k (d_j^+ + d_j^-) \\ \text{s.t.} : & f_j(\mathbf{X}) + d_j^+ + d_j^- = b_j, \quad d_j^+, d_j^- \geq 0, \quad d_j^+ d_j^- = 0, \quad j = 1 \dots k \end{aligned} \tag{15}$$

Because the goal is predetermined before optimization in this study, it is easy to assess whether the predetermined goal has been reached. This is the main reason why GP was used rather than the multiobjective GA or other methods. The whole process of the fatigue optimization of the end beam in the bogie frame is illustrated in Fig. 7.

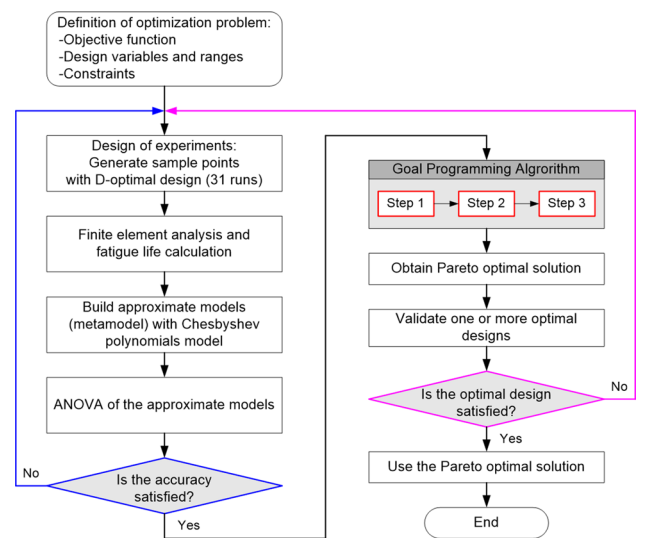


Fig. 7 Flowchart of the fatigue optimization

5 Multiobjective Optimization Results

5.1 Design Objectives and Variables

Five sizes ranging from x_1 to x_5 were taken as the design variables. The initial values and ranges/levels of the five design variables are presented in Table 2 and Fig. 8. The ranges of the design variables were defined by the equidistance relative to their baseline values.

5.2 Optimization Formulation

For this multiobjective optimization, maximizing the fatigue life and minimizing the maximum stress, as well as minimizing the weight of the end beam, are considered as the design objectives. Thus, the optimization problem can be formulated as follows:

$$\begin{cases} \text{Find} : X(x_1, \dots, x_5) \\ \left\{ \begin{array}{l} \text{Max} : f_{N_f} \\ \text{Min} : f_{stress} \\ \text{Min} : f_{weight} \end{array} \right. \\ \text{s.t.} : x_{iL} \leq x_i \leq x_{iU} \quad i = 1, \dots, 5 \end{cases} \tag{16}$$

Among these three design objectives, the objective having the highest priority is (1) Increasing the fatigue life, followed by (2) Reducing the maximum stress and (3) Reducing the

Table 2 Optimal configuration of the design parameters with changes in the baseline values

Design variations	Initial value	Range	
		Lower	Upper
Channel thickness (x_1)	9 mm	7 mm	11 mm
Channel thickness (x_2)	9 mm	7 mm	11 mm
Channel thickness (x_3)	7.5 mm	5 mm	10 mm
Gusset plate length (x_4)	250 mm	100 mm	400 mm
Gusset plate position (x_5)	710 mm	680 mm	740 mm

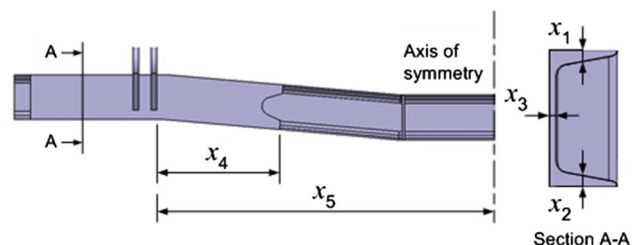


Fig. 8 Design variables of the end beam

frame weight, according to priority order of the objectives. The required levels for the design objectives are set at the beginning of the design and are as follows:

$$\begin{cases} f_{N_f}^* = 10.0^6 \text{ cycle} \\ f_{stress}^* = 52.0 \text{ MPa} \\ f_{weight}^* = 35.0 \text{ Kg} \end{cases} \quad (17)$$

In this procedure, after the satisfactory level is set for each objective, the objective having the highest priority is optimized first, followed by the objective having the second priority. Then, the procedure is repeated for every objective in order of its priority. The optimal solution in each design stage is obtained using a feasible direction method.

5.3 DOE

A total of 31 sample points were generated using D-optimal design, which were considered adequate for evaluating 20 coefficients of the Chebyshev polynomial model with five design variables. Table 3 presents the 31 runs and the corresponding results at the sampling points.

5.4 Chebyshev Polynomials and ANVOA

After the experimental results in Table 3 were obtained, the approximate models of the objective functions were constructed in the linear function with the interaction of each other, as follows:

Table 3 Layout and data for D-optimal design

No	x ₁	x ₂	x ₃	x ₄	x ₅	Stress (MPa)	Weight (kg)
1	1	3	2	3	1	74.50	35.75
2	1	1	3	3	3	75.29	36.50
3	3	2	3	1	3	62.75	37.81
4	3	1	3	1	1	64.18	36.50
5	2	3	2	2	2	74.34	35.85
6	1	1	1	2	1	128.67	28.16
7	1	3	3	1	3	64.65	36.50
8	1	1	2	1	1	103.25	30.36
9	3	3	3	3	3	53.85	41.69
10	3	2	2	2	2	77.04	35.85
11	1	1	1	2	1	123.43	28.16
12	1	3	1	3	3	65.13	32.41
13	3	1	1	3	3	89.11	32.41
14	3	3	1	1	1	74.18	32.78
15	1	3	1	1	1	119.30	29.81
16	3	3	3	1	1	54.64	39.13
17	1	1	1	1	3	125.49	26.84
18	1	1	2	1	1	94.99	30.54
19	3	3	3	3	1	50.20	41.69
20	1	2	3	3	1	71.48	37.80
21	1	1	3	1	2	100.55	33.87
22	1	1	1	3	2	88.48	29.47
23	3	3	1	1	3	69.74	32.78
24	3	1	3	3	1	52.42	39.10
25	2	3	2	2	2	68.87	39.11
26	3	1	1	3	1	77.36	32.41
27	3	3	1	3	1	87.05	35.35
28	1	3	3	1	1	79.49	36.50
29	3	2	2	2	2	66.56	35.85
30	1	3	2	3	1	67.67	35.75
31	3	1	1	1	1	83.08	29.81

$$\begin{aligned}
 f_{stress} = & -3080 - 86.41x_1 + 93.93x_2 - 68.97x_3 + 2.7427 + 0.0808x_4 \\
 & - 0.001008 - 7.468x_5 + 0.005314 + 0.4258x_1x_2 \\
 & + 0.024954x_1x_4 + 0.09918x_1x_5 - 0.4824x_1x_3 + 0.015682x_2x_4 \\
 & - 0.14618x_2x_5 + 0.03680x_3x_5
 \end{aligned}
 \tag{18}$$

$$\begin{aligned}
 f_{weight} = & -59 + 12.022x_1 - 0.62919 + 0.9851x_2 - 0.01607 \\
 & + 1.4618x_3 + 0.00885 + 0.004897x_4 + 0.000007 + 0.0539x_5 \\
 & - 0.000038
 \end{aligned}
 \tag{19}$$

Equations (6) was used to determine the fatigue life of the end beam. The fatigue notch factor K_f of the end beam was calculated using Eqs. (1)–(3), and its value was 1.3375. The fatigue life of the end beam was predicted by using the stress corrected using the fatigue notch factor K_f and P–S–N curve in Fig. 2. Equation (20) gives the ANVOA and approximation model for the fatigue life of the end beam.

$$\begin{aligned}
 f_{N_f} = & -1384963 + 797718x_1 - 1022452x_2 + 461933x_3 - 15263 \\
 & - 854x_4 + 7.098 + 768x_5 + 612345x_1x_3 - 153.77x_1x_4 \\
 & - 1116.9x_1x_5 + 7201x_2x_3 - 145.96x_2x_4 + 1504.3x_2x_5 + 76.14x_3x_4 \\
 & - 506.1x_3x_5
 \end{aligned}
 \tag{20}$$

Tables 4, 5, 6 present the ANOVA results for the fitted models. The total errors between the surrogate model and the computer analysis, i.e., R^2 for f_{N_f} , f_{stress} , and f_{weight} , were 3.04%, 2.41%, and 0.35%, respectively, Hence, the accuracies of the approximation models were considered to be adequate for the present study.

5.5 Multiobjective Optimization Using GP

With GP, the entire optimization process can be divided into three steps for the three design variables. In each step, one objective is selected as the objective/cost function, and other two are used as constraints. The process is described as follows. The multiobjective optimization problem is turned into a constrained single-objective problem in this step, because maximizing the fatigue life is the first preference in this study.

Step 1:

Table 4 ANOVA results for the model fitted to f_{N_f}

Model	SS	DOF	MS	F	P
Regression	2.58649E+12	1	2.58649E+12	923.41	0
Residual	81,229,620,954	29	2,801,021,412		
Total	2.66772E+12	30			

Table 5 ANOVA results for the model fitted to f_{stress}

Model	SS	DOF	MS	F	P
Regression	24,472	1	24,472	1176.15	0
Residual	603	29	21		
Total	25,075	30			

$$\begin{cases}
 \text{Max. } f_{N_f} \\
 \text{S.t. } \begin{cases}
 f_{stress} \leq 52 \\
 f_{weight} \leq 35 \\
 x_{iL} \leq x_i \leq x_{iU} \quad i = 1 \dots 5
 \end{cases}
 \end{cases}
 \tag{21}$$

Here, $f_{fatigue}^* < f_{fatigue}^e$, that is, the maximum value of the objective function $f_{fatigue}$ does not satisfy the required hard

objective level $f_{fatigue}^e$, and the designers can relax the set values of the required soft objective levels f_{stress}^e and f_{weight} and return the process to step (1). If $f_{fatigue}^* > f_{fatigue}^e$, the deviation Δ_1 is defined as the allowable limit for the relaxation range of $f_{fatigue}$. Because two relaxations for $f_{fatigue}$ are required after the maximization of $f_{fatigue}$, the deviation Δ_1 can be estimated using the following equation.

$$\Delta_1 = \left| \frac{f_{fatigue}^e - f_{fatigue}^*}{2} \right|
 \tag{22}$$

The minimum value f_{stress}^* of the objective function f_{stress} corresponding to the hard objective having the second priority is obtained by solving the following problem.

Step 2:

$$\begin{cases}
 \text{Min. } f_{stress} \\
 \text{S.t. } \begin{cases}
 f_{N_f} \leq 1,194,300 + 97,150.40 \\
 f_{weight} \leq 35 \\
 x_{iL} \leq x_i \leq x_{iU} \quad i=1 \dots 5
 \end{cases}
 \end{cases}
 \tag{23}$$

Table 6 ANOVA results for the model fitted to f_{weight}

Model	SS	DOF	MS	F	P
Regression	467.91	1	467.91	1992.75	0
Residual	6.81	29	0.23		
Total	474.72	30			

Table 7 Comparison between optimum and reanalysis results

Solution	Fatigue life (cycle)	Stress (MPa)	Weight (kg)
Initial	603,095	75.4	28.4
Optimum	1,277,000	39.4	33.4
Reanalysis	1,231,000	42.1	34
Error (%)	3.5	4.9	1.8

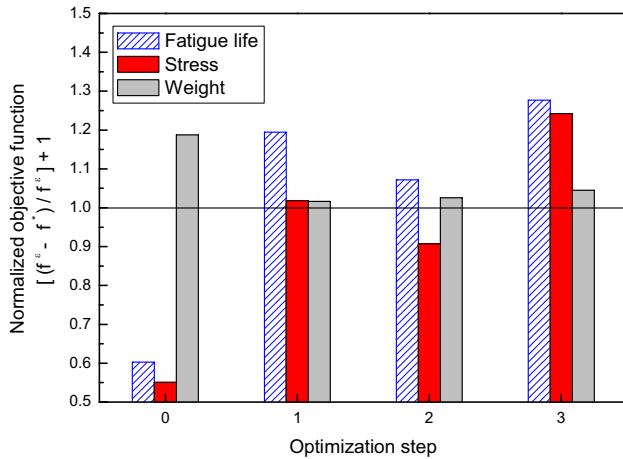


Fig. 9 Optimization step vs. normalized objective function

where $f_{stress}^* > f_{stress}^e$, that is, the minimum value of the objective function, f_{stress} , does not satisfy the required hard objective level f_{stress}^e . The designers can relax the set values of the required soft objective levels $f_{fatigue}^e$ and f_{weight}^e and try again. If $f_{stress}^* < f_{stress}^e$, the deviation Δ_2 is defined as the allowable limit for the relaxation range of f_{stress} . Because two relaxations for f_{stress} are required after the maximization of f_{stress} , the deviation Δ_2 can be estimated using the following equation.

$$\Delta_1 = \left| \frac{f_{stress}^e - f_{stress}^*}{2} \right| \tag{24}$$

Similarly, minimization of the frame weight should be performed successively by solving the following problem. Step 3:

$$\begin{cases} \text{Min. } f_{weight} \\ \text{S.t. } \begin{cases} f_{N_f} \leq 1,194,300 + 97,150.40 \\ f_{stress} \leq 56.84 + 2.42 \\ x_{iL} \leq x_i \leq x_{iU} \quad i=1\dots5 \end{cases} \end{cases} \tag{25}$$

Table 7 presents the final updated values obtained in the foregoing steps for each objective function. Clearly, all the required objective levels are satisfied.

Figure 9 shows the normalized objective functions obtained during three optimization cycles. The normalized objective function f is defined as follows:

$$f = \left[\frac{(f^e - f^*)}{f^e} + 1 \right] \tag{26}$$

where f^* represents the optimum value at each stage, and f^e represents the required objective-function value. If the normalized objective function exceeds 1, the objective function satisfies the constraints. At the initial design stage, fatigue life and stress do not exist in a feasible design space, except for weight. This is because the relative importance between objective functions is not estimated quantitatively, and there is significant reliance on the intuition of the designer. The final optimization results indicate that all the objective functions satisfy all the objective levels.

In Table 7, the objectives verified by FEA are compared with those predicted by the fitted model. The estimated optimal solutions are also verified by the FEA solutions within the tolerance error. The difference between the verified and the estimated objective functions is due to the error from the structural analysis and approximation. Clearly, the bogie frame optimized using priority ranking design optimization has better performance than that obtained using the primitive design model.

6 Conclusions

Fatigue optimization was examined for a brake end beam of the bogie frame, which is widely used in freight trains. FEAs were performed instead of real experiments, which are typically expensive and unprintable. The fatigue life was calculated using the stress-life curve method, with consideration of the notch influence. For the optimization, the fatigue life, stress, and weight of the end beam were taken into account simultaneously (as a multiobjective optimization problem). The Chebyshev polynomial response surface model was adopted for approximating the response functions. The GP method was used to search for the Pareto-optimal solution. The results indicated that the fatigue life was significantly increased compared with the initial design, while the stress and weight were both reduced; i.e., compared with the initial structure, the optimized end beam structure had better safety performance and was lighter.

The proposed approach is suitable and effective for the fatigue optimization problem, which is usually time-consuming owing to the difficult fatigue analysis and three

different criteria. Our method can be used for the optimal design of bogie frames under complex working conditions.

References

- Okamoto I (1998) How bogies work. *Jpn Railw Transp Rev* 18:52–61
- Dietz S, Netter H, Sachau D (1998) Fatigue life prediction of a railway bogie under dynamic loads through simulation. *Veh Syst Dyn* 29(6):385–402
- Oyan C (1998) Structural strength analysis of the bogie frame in Taipei rapid transit systems. *Proc Inst Mech Eng Part F J Rail Rapid Transit* 212(3):253–262
- Ferguson NS (2000) Modelling the vibrational characteristics and radiated sound power for a Y25-type bogie and wagon. *J Sound Vib* 231(3):791–803
- Kim JS, Kim NP (2007) Evaluation of structural safety of a tilting bolster. *Eng Fail Anal* 14(1):63–72
- Baek SH, Cho SS, Joo WS (2008) Fatigue life prediction based on the rainflow cycle counting method for the end beam of a freight car bogie. *Int J Autom Technol* 9(1):95–101
- Barsoum Z, Lundback A (2009) Simplified FE welding simulation of fillet welds-3D effects on the formation residual stresses. *Eng Fail Anal* 16(7):2281–2289
- Kim JS, Yoon HJ (2011) Structural behaviors of a GFRP composite bogie frame for urban subway trains under critical load conditions. In: 11th International Conference on the Mechanical Behavior of Materials (ICM11), Como, Italy
- Jeon KW, Shin KB, Kim JS (2011) A study on fatigue life and strength of a GFRP composite bogie frame for urban subway trains. In: 11th International Conference on the Mechanical Behavior of Materials (ICM11), Como, Italy
- Kassner M (2012) Fatigue strength analysis of a welded railway vehicle structure by different methods. *Int J Fatigue* 34(1):103–111
- Esderts A, Willen J, Kassner M (2012) Fatigue strength analysis of welded joints in closed steel sections in rail vehicles. *Int J Fatigue* 34(1):112–121
- Latos W, Zyczkowski M (1973) The optimum of rotating shaft for combined fatigue strength. *Acad Pol Sci Bull Ser Sci Tech* 21(8):523–533
- Park BH, Kim NP, Kim JS, Lee KY (2006) Optimum design of tilting bogie frame in consideration of fatigue strength and weight. *Veh Syst Dyn* 44(12):887–901
- Wang HY, Kim NH, Kim YJ (2006) Safety envelope for load tolerance and its application to fatigue reliability design. *J Mech Des* 128(4):919–927
- Mrzyglod M, Zielinski AP (2007) Parametric structural optimization with respect to the multiaxial high-cycle fatigue criterion. *Struct Multidiscip Optim* 33(2):161–171
- Mrzyglod M, Zielinski AP (2007) Multiaxial high-cycle fatigue constraints in structural optimization. *Int J Fatigue* 29(9–11):1920–1926
- Song XG, Jung JH, Son HJ, Park JH, Lee KH, Park YC (2010) Metamodel-based optimization of a control arm considering strength and durability performance. *Comput Math Appl* 60(4):976–980
- Bosnjak S, Petkovic Z, Zrnic N, Pantelic M, Obradovic A (2010) Failure analysis and redesign of the bucket wheel excavator two-wheel bogie. *Eng Fail Anal* 17(2):473–485
- Japanese Standards Association (1984) Japanese Industrial Standard (JIS) E4207, Truck frames for railway rolling stock-general rules for design.
- Atkinson AC, Donev AN (1989) The construction of exact D-optimum experimental designs with application to blocking response surface designs. *Biometrika* 76(3):515–526
- Box GEP, Hunter WG, Hunter JS, Hunter WG (1978) Statistics for experimenters: an introduction to design, data analysis and model building. Wiley, New York
- Lee CP, Huang MNL (2011) D-Optimal designs for second-order response surface models with qualitative factors. *J Data Sci* 9:139–153
- Montgomery DC (2008) Design and analysis of experiments. Wiley, New York
- Das I, Dennis JE (1997) A closer look at drawbacks of minimizing weighted sums of objectives for Pareto set generation in multicriteria optimization problems. *Struct Optim* 14(63–69):1–13
- Floudas CA, Pardalos PM, Adjiman CS, Esposito WR, Gümüs ZH, Harding ST, Klepeis JL, Meyer CA, Schweiger CA (1999) Handbook of test problems in local and global optimization. Kluwer Academic Publishers, Dordrecht/Boston/London
- Marler RT, Arora JS (2004) Survey of multi-objective optimization method for engineering. *Struct Multidiscip Optim* 26:369–395
- Ming Z, Wang G, Yan Y, Panchal JH, Goh CH, Allen JK, Mistree F (2018) Ontology-based representation of design decision hierarchies. *ASME J Comput Inf Sci Eng* 18(1):011001
- Jafaryeganeh H, Ventura M, Guedes Soares C (2020) Effect of normalization techniques in multi-criteria decision making methods for the design of ship internal layout from a Pareto optimal set. *Struct Multidiscip Opt* 62:1849–1863

Publisher's Note Springer Nature remains neutral with regard to jurisdictional claims in published maps and institutional affiliations.

Seokheum Baek is a Senior Manager at DNDE Inc., Korea. He received his BS, MS and Ph.D. degrees in Mechanical Engineering from Dong-A University, Korea, in 2001, 2003, and 2010, respectively. His current research interests include optimization and uncertainty quantification, field metamodeling and data science in design, turbine and power engineering.

Xueguan Song is a Professor at Dalian University of Technology, China. He received his BS degree in mechanical engineering from the Dalian University of Technology, China, in 2004, and the MS and Ph.D. degrees in mechanical engineering from Dong-A University, Korea, in 2007 and 2010, respectively. His research interests include multidisciplinary design optimization, numerical modeling, data analysis, and data-driven design.

Myungil Kim is a Principal Researcher at Korea Institute of Science and Technology Information (KISTI), Korea. He received his BS, MS and Ph.D. degrees in Computer Science and Engineering from Chungang University, Korea, in 1998, 2000, and 2004, respectively. His current research interests include modeling and simulation, cloud computing, supercomputing and research network.

Jaesung Kim is a Assistant Professor at Hanbat National University, Korea. He received his MS and Ph.D. degrees in Industrial Engineering from Pohang University of Science and Technology (POSTECH), Korea, in 1999, and 2003, respectively. His current research interests include modeling and simulation, manufacturing data analysis and digital twin.